THE JOURNAL OF PHYSICAL CHEMISTRY C

ARTICLE

pubs.acs.org/JPCC

Nanoscale Structure of Ionic Liquid and Diffusion Process as Studied by the MFE Probe

Tomoaki Yago and Masanobu Wakasa*

Department of Chemistry, Graduate School of Science and Engineering, Saitama University, 255 Shimo-ohkubo, Sakura-ku, Saitama, 338-8570, Japan

Supporting Information

ABSTRACT: Magnetic field effects (MFEs) observed for photoinduced hydrogen abstract reaction between benzophenone and thiophenol, generating phenylthiyl and benzophenone ketyl radicals, in an ionic liquid of *N,N,N,*-trimethyl-*N*-propylammonium bis(trifluoromethanesulfonyl)amide (TMPA TFSA) were analyzed by using the stochastic Liouville equation (SLE) with the cage model and the solvent separated radical pair model, respectively. The MFEs observed on the yield of escaped benzophenone ketyl radical in the range of $0 < B \leq 2.0$ T were explained by the transverse spin relaxation in the radical pair caused by the large anisotropy of the *g*-value and the slow rotation of phenylthiyl radical in the IL. The calculated MFE was dependent on a rotational correlation time of the radical as well as the mutual diffusion coefficient for the translational diffusion of the radicals. The SLE analysis revealed that the IL has at least two different viscosity regions, causing the nanoscale cage effect on the radical diffusion in the IL.

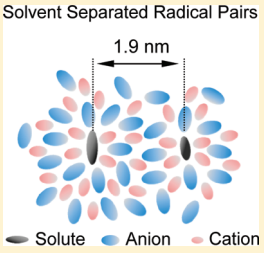

INTRODUCTION

Ionic liquids (ILs) are currently promising new class of solvents in green chemistry, electrochemistry, and nanochemistry.[1−7] Compared with conventional organic solvents, ILs are nonvolatile, noncorrosive, nonflammable, stable in air and moisture, and designable. Such properties of ILs provide new environments for chemical reactions. Thus, ILs have been applied to many fields such as catalysis, synthesis, electron transportation, polymerization, and formation of nanomaterials. Although a number of studies on their structures and functions have been reported,[8−11] the mechanistic insight into chemical reactions in ILs is still unclear because of the complex solvent structures in ILs. Especially, it has been reported that the ILs have nanoscale ordering structures as a result of the strong coulombic interactions and the aggregation of the nonpolar parts of ionic molecules.[9−11] One of the most controversies regarding the nanoscale ordering structures is the solute molecular diffusion in ILs. Several time-resolved optical studies reported that the rate constants of chemical reactions in ILs were much higher than those of the diffusion-controlled chemical reaction predicted from the macroviscosity of ILs, suggesting the microviscosities in the vicinity of reactants are different from the macroviscosities in the ILs.[12−15]

To study such fast diffusion motions of molecules in the nanoscale ordering structures, we have developed the magnetic field effect probe (MFE probe), which can clarify the microenvironment by observing magnetic field effects (MFEs) on photochemical reactions through radical pairs (RPs).[16] Magnetic fields interact with the electron spins of RPs, and thus the spin conversion in the RPs is influenced by the fields. The lifetime of the RPs and the yield of the escaped radicals show appreciable MFEs.[17−19] Because the interactions of electron spins in RPs are limited to within a few nanometers, the MFE probe are sensitive to the microenvironment around the RP. Thus, one can probe the radical diffusion in the nanoscale structure by the MFE probe. In our previous study,[16] the MFEs on the photoinduced hydrogen abstraction reaction of benzophenone (BP) with thiophenol (PhSH) were observed in alcoholic solutions of varying viscosities from 0.55 to 59.2 cP. The hydrogen abstraction reaction to generate the RP can be represented as follows:

$$\mathrm{BP} + \mathrm{PhSH} \xrightarrow{h\nu} {}^{3}\mathrm{BP}^{*} + \mathrm{PhSH} \rightarrow {}^{3}(\mathrm{BPH}\cdot\cdot\mathrm{SPh}) \qquad (1)$$

where ^{3}BP* represents the triplet excited state of BP. BPH· and ·SPh represent the benzophenone ketyl and phenylthiyl radicals, respectively. The observed MFEs were sensitive to the solvent viscosity and the detailed analysis by the stochastic Liouville equation (SLE) showed that the MFEs were associated with the microviscosity in the vicinity of the RP rather than the macroviscosity of the solvents. Using a technique similar to that of MFEs, more recently Maeda et al. reported protein surface interactions of hen egg white lysozyme (HEWL).[20] Thus, the MFE probe is a powerful technique to clarify molecular diffusions and interactions in the microenvironment.

The MFE probe was very recently applied to study the molecule diffusions and nanosacale structures in ILs.[21−23] In an IL of *N,N,N*-trimethyl-*N*-propylammonium bis(trifluoromethanesulfonyl) amide (TMPA TFSA), we have observed the large MFEs for the photoinduced hydrogen abstraction reaction of BP with PhSH in TMPA TFSA in the range of $0 T < B \leq 28$ T. The observed MFEs have the following characteristics: (1) The escape yield of BPH· generated from the hydrogen abstraction reaction decreased with increasing *B* in the range of $0 T < B \leq 2$ T. The decrease was almost saturated for

Received: November 14, 2010
Revised: December 24, 2010
Published: January 20, 2011

ACS Publications © 2011 American Chemical Society

dx.doi.org/10.1021/jp1108762 | *J. Phys. Chem. C* 2011, 115, 2673–2678

2 $T < B \leq 10$ T, giving the 78% decrease in the escaped yield of BPH· at 10 T.[22] The observed MFEs were preliminarily analyzed by the SLE and the RPs generated from the reaction were found to be confined in a nanoscale cage with the radius of 1.8 nm and the effective viscosity of 1−2 cP in the cage of the IL.[23] However, the details of nanoscale inhomogeneous structure of the IL and molecular diffusion in the IL have not been reported. In this article, we provide a full description of the theoretical analysis on the MFEs observed in the IL by using the SLE.

METHOD

In the present study, the analysis by the SLE includes the effects of spin−spin interactions, molecular diffusion, recombination reactions at the contact RP, and spin relaxations. The details of the SLE analysis are described in the Supporting Information.

The spin Hamiltonian is composed of the Zeeman interactions for the radicals, the hyperfine interactions between electron and nuclear spins with a hyperfine coupling constant (A), and the exchange interaction (J), which is dependent on the radical−radical distance (r). The diffusion of the radicals was assumed to proceed by a simple Brownian motion and was treated by the finite difference technique with mutual diffusion coefficient D. The recombination reactions are proceeded from the contact RP.

In confined systems where the lifetimes of RPs are comparable with the spin relaxation times, the spin relaxations play an important role on the spin conversion in RPs.[19] The rate constants for the spin relaxations depend on the magnitude of the fluctuating local magnetic field and the frequency for the fluctuation represented with the rotational correlation time (τ). The spin relaxations by the anisotropy (δA) of the hyperfine interaction, the anisotropies (δg) of the g-factors, the dipole−dipole interactions, and the spin rotational interactions were taken into account. The longitudinal relaxation rate constant ($1/T_1$) is represented as,[19,28]

$$\frac{1}{T_1} = \frac{3(g_a':g_a')\mu_B{}^2B^2 + (A':A')}{30\hbar^2} \times \frac{\tau_a}{1+\omega^2\tau_a{}^2} + \frac{3(g_b':g_b')\mu_B{}^2B^2}{30\hbar^2} \times \frac{\tau_b}{1+\omega^2\tau_b{}^2} + \frac{1}{T_{SR}} \quad (2)$$

where $(g':g')$ and $(A':A')$ are the magnitudes of the anisotropies for the g-factor and the hyperfine coupling constant, respectively. ω is the Larmor frequency for the unpaired electron spin and is dependent on magnetic field strength B; $\omega = g\,\mu_B\hbar^{-1}B$. τ_a and τ_b are rotational correlation times for radical a and b, respectively. T_{SR} is the relaxation time due to the spin-rotational interaction. In the presence of the large J value in the closed RP, the transverse relaxation rate constant ($1/T_2$) for the $S-T_0$ relaxation is represented as,

For $2J(r) > \{[3(g_a':g_a')\,\mu_B{}^2B^2+(A':A')]/30\hbar^2\}^{1/2}$,

$$\frac{1}{T_2} = \frac{3(g_a':g_a')\mu_B{}^2B^2 + (A':A')}{30\hbar^2} \times \frac{\tau_a}{1+[2J(r)]^2\tau_a{}^2} + \frac{3(g_b':g_b')\mu_B{}^2B^2}{30\hbar^2} \times \frac{\tau_b}{1+[2J(r)]^2\tau_b{}^2} + \frac{1}{T_{SR}} \quad (3)$$

When the S and T_0 states are nearly degenerated, on the other hand, $1/T_2$ is represented as,

Table 1. Magnetic and Kinetic Parameters for Radical Pairs Used for SLE Analysis[a]

parameters	used values
J_0	-1×10^{12} rad s^{-1}
β	20 nm^{-1}
d_a	0.4 nm
d_b	0.2 nm
k_{rec}	5×10^{10} s^{-1}
k_{SOC}	4×10^{9} s^{-1}
A	−0.4 mT
δA	0.2 mT
g_a	2.003
g_b	2.0082
δg_a	0.002
δg_b	0.02

[a] Determined in ref 16.

Scheme 1. Two Models Used in the SLE Analysis

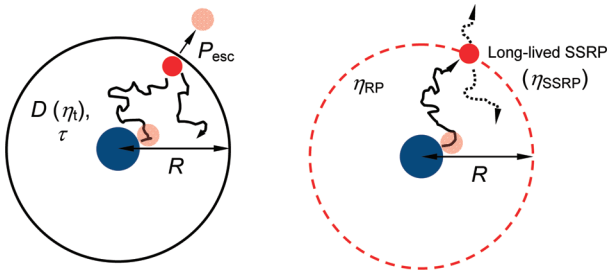

For $2J(r) < \{[3(g_a':g_a')\,\mu_B{}^2B^2+(A':A')]/30\hbar^2\}^{1/2}$,

$$\frac{1}{T_2} = \frac{1}{T_2'} + \frac{1}{2T_1} \quad (4)$$

$$\frac{1}{T_2'} = \frac{3(g_a':g_a')\mu_B{}^2B^2 + (A':A')}{30\hbar^2} \times 4\tau_a + \frac{3(g_b':g_b')\mu_B{}^2B^2}{30\hbar^2} \times 4\tau_b + \frac{1}{T_{SR}} \quad (5)$$

In the SLE analysis, we assumed that the RP was initially populated with the three triplet states (T_+, T_0, T_-) equally at the closest distance d. The most of the parameters needed for the SLE analysis have been fixed by fitting the MFEs data obtained for the same photochemical reaction in the various alcoholic solvents.[16] The fixed parameters are listed in Table 1.

The parameters discussed in the present study are associated with two models depicted in Scheme 1. Cage model is a model where RPs are confined in spherical cage with radius R.[32] At the boundary, RP are escaped from the cage with the probability P_{esc}. The P_{esc} value is defined as k_{out}/k_{in}, where k_{out} and k_{in} are escape rate and reflection rate at the boundary of the cage, respectively. In this model, as mentioned later, parameters of D and the rotational correlation times (τ_a and τ_b) for radicals are not correlated. Once the radicals escape from the cage, the radical cannot diffuse back inside of the cage.

dx.doi.org/10.1021/jp1108762 |J. Phys. Chem. C 2011, 115, 2673–2678

A solvent separated radical pair (SSRP) model is a model where the SSRP with a specific radical−radical distance (R) are stable and have the longer lifetime.[33] The viscosity (η_{SSRP}) effective for the SSRP is different from the viscosity (η_{RP}) for the other RPs. The τ_a and τ_b values, and the lifetime of the SSPR are determined by the η_{SSRP} value. The other RPs diffuse with the viscosity of η_{RP}. Thus the RPs feel the two different viscosities in the course of diffusion. In this model, we assumed that the Stokes−Einstein and the Stokes−Einstein−Debye relationships are always held for the translational diffusion and the rotational motion of solute radicals, respectively.

$$D_a(\eta) = \frac{k_B T}{6\pi\eta d_a}; D_b(\eta) = \frac{k_B T}{6\pi\eta d_b} \quad (6)$$

$$\tau_a = \frac{4\pi\eta {d_a}^3}{3k_B T}; \tau_b = \frac{4\pi\eta {d_b}^3}{3k_B T} \quad (7)$$

where d_a and d_b are the radius of each radical, respectively. Nishiyama et al. reported that the diffusion of radicals in ILs can be described by the Stokes−Einstein relationships with the stick boundary condition from the transient grating measurement.[35] For the radius of solute molecules, we used the value of d_a = 0.4 nm for BPH· and d_b = 0.2 nm for PhS·. These values were obtained by the diffusion coefficient for the same or similar radicals in organic solvents.[36,37] We assumed that, once the radicals escape from the SSRP, the RP does not form again in the calculations.

RESULTS AND DISCUSSION

In general, the MFEs due to the radical pair mechanism (RPM) are observed during sequential steps as follows: (1) formation of close RPs through photochemical reactions with singlet (S) or triplet (T_n, n = 0, ±1) spin multiplicity, (2) spin conversion between S and T_n states in separated RPs where S and T_n states are nearly degenerated, and (3) spin-state selective recombination of the close RPs competing with the escape of radicals from the pairs. These steps are promoted by the diffusion of the radicals by which the RPs are separated and re-encountered. Because the interactions of electron spins in RPs are limited to within a few nanometers, the MFEs reflect the spin dynamics of the RP where the radicals are separated at a few nanometers. The observations of the large MFEs in the present photochemical reaction, therefore, imply an existence of the nanometer separated RPs in the IL.

Because the MFEs were saturated at $2T < B$, the SLE analysis converged on the MFEs obtained at the magnetic fields lower than $2T$. The calculated yields of the escaped radical, $R_{calcd}(B)$, using the cage model, are shown in Figure 1 together with the experimental data (filled circles). As was reported in the previous study,[23] the experimental data were well reproduced by the SLE calculations (red line) with the parameters of R = 1.8 nm, $P_{esc} = 8 \times 10^{-4}$, $D = 1.6 \times 10^{-9}$ m^{2}s^{-1} (= 1−2 cP from the Stokes−Einstein relationship), and $\tau_a = \tau_b$ = 5 ns, as shown in Table 2. To clarify the contribution of the transverse spin relaxations due to δg_b on the MFEs, $R_{calcd}(B)$ was also calculated in the absence of the transverse spin relaxation. The results (blue line) are also shown in Figure 1. In the absence of the transverse spin relaxation, R_{calcd} does not decrease with increasing B and the SLE calculations could not reproduce the experimental data. From eqs 4 and 5, the transverse spin relaxation time of the present RP is estimated to be 30 ns at 0.1 T, 320 ps at 1 T, and 80 ps at 2 T with the value of $\tau_a = \tau_b$ = 5 ns. Thus the observed

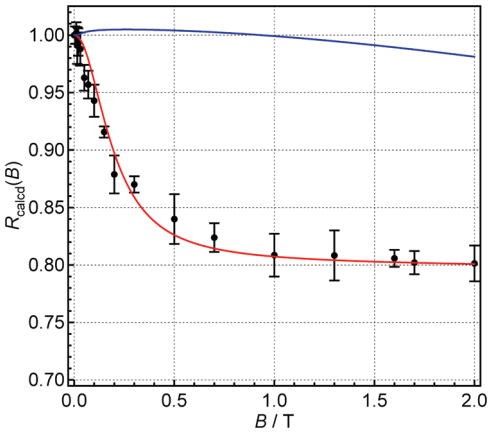

Figure 1. $R_{calcd}(B)$ calculated by the cage model in the presence of the transverse spin relaxation (red line, δg_b = 0.02) and in the absence of the transverse spin relaxation (blue line, δg_b = 0). Parameters used in the calculations are listed in Tables 1 and 2. Filled circles are corresponding experimental results obtained in TMPA TFSA.

Table 2. Parameters for Radical Pair Diffusions Used in the SLE Analysis

model	parameters	used values
cage model	R	1.8 ± 0.3 nm[a]
	P_{esc}	8×10^{-4}[a]
	D	1.6×10^{-9} m^{2}s^{-1}[a]
	τ_a, τ_b	5 ns [a]
SSRP model	R	1.9 ± 0.5 nm
	η_{RP}	4 cP
	η_{SSRP}	2800 cP

[a] Ref 23.

MFEs are mainly explained by the magnetic field dependent transverse spin relaxation between the S and T_0 states, which is caused by the large δg_b and the long τ_b values for ·PhS. The transverse spin relaxation caused by BPH· has little effect on $R_{calcd}(B)$ due to the small δg_a value. Hansen and Pedersen have also reported that the transverse and longitudinal spin relaxations caused by δg affects the MFEs in the similar photochemical reaction of 4-methoxybenzophenone with PhSH.[38]

The transverse spin relaxation process is influenced by the rotational correlation time (τ) in accordance with eq 5. The MFEs are therefore expected to be dependent on the τ values. Next, to investigate the effect of τ on the MFEs, $R_{calcd}(B)$ were calculated with various τ values. Because the δg_a value is small and the transverse spin relaxation by BPH· has little effect on $R_{calcd}(B)$, the τ_a value also has little effect on $R_{calcd}(B)$. We therefore assumed that τ_a is the same as τ_b for simplicity. The obtained results are shown in Figure 2. With increasing τ_b, the transverse spin relaxation is accelerated at the all magnetic fields except the zero-magnetic field in accordance with eq 5. As a result, the saturation field of $R_{calcd}(B)$ decreases with increasing τ_b. The results indicate that nanosecond ordered τ_b value for ·PhS is necessary to reproduce the experimental data.

Our previous MFEs study in the homogeneous solutions shows that the MFE for the present reaction is sensitive to the microviscosity in the vicinity of RPs and the translational diffusion motion of radicals can be probed by observing the MFEs.[16] In this study, we therefore investigated how the MFE with the

dx.doi.org/10.1021/jp1108762 |J. Phys. Chem. C 2011, 115, 2673–2678

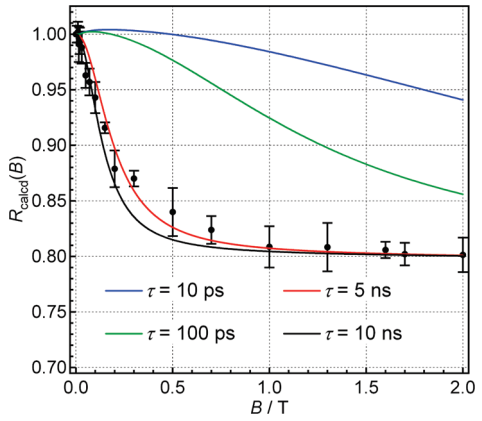

Figure 2. $R_{calcd}(B)$ calculated by the cage model with the parameters of $\tau_a = \tau_b = 1 \times 10^{-11}$ s (blue), $\tau_a = \tau_b = 1 \times 10^{-10}$ s (green), $\tau_a = \tau_b = 5 \times 10^{-9}$ s (red), and $\tau_a = \tau_b = 1 \times 10^{-8}$ s (black). Other parameters used in the calculations are listed in Tables 1 and 2. Filled circles are corresponding experimental results obtained in TMPA TFSA.

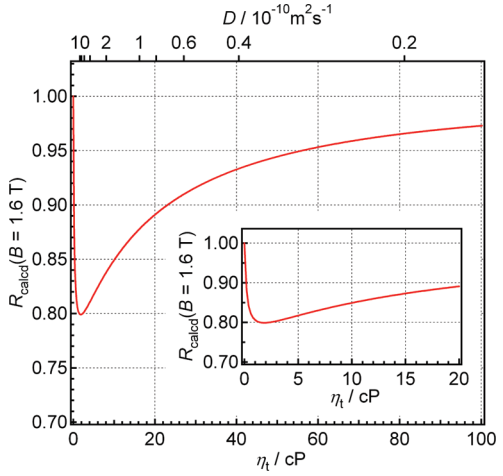

Figure 3. η_t dependence of $R_{calcd}(B)$ calculated at magnetic field of 1.6 T by the cage model. η_t is a viscosity effective for the translational diffusion of radicals in the cage. Other parameters used in the calculations are listed in Tables 1 and 2. Insert shows detail of data at the lower η_t values.

cage model is affected by the radical translational diffusion in the cage. For convenience, the translational diffusion motion of the radical is represented by viscosity (η_t) instead of D in the analysis. Here, η_t is defined as a viscosity effective for the translational diffusion of radicals in the cage and correlated with D by the Stokes−Einstein relationship (eq 6). The η_t dependence of $R_{calcd}(B)$ was calculated at 1.6 T by the cage model with fixed values of $P_{esc} = 8 \times 10^{-4}$, $\tau_a = \tau_b = 5$ ns as shown in Figure 3. R_{calcd}(1.6 T) decreased with increasing η_t, in the range of 0 cP < B < 2 cP, and then increased with increasing η_t in the range of 2 cP < B < 100 cP. Such reversion of R_{calcd}(1.6 T) can be explained by the strong spin−orbit coupling effect in highly viscous region.[16] The SLE calculations with the cage model indicate that the MFE on the present reaction in IL is enough sensitive to D and η_t to find the reverse future on the $R_{calcd}(B)$ values. When the calculations were performed with the fixed P_{esc} and R values, the magnitude of the MFEs are mainly determined by the D and η_t values whereas the τ value determines the shape of the MFE

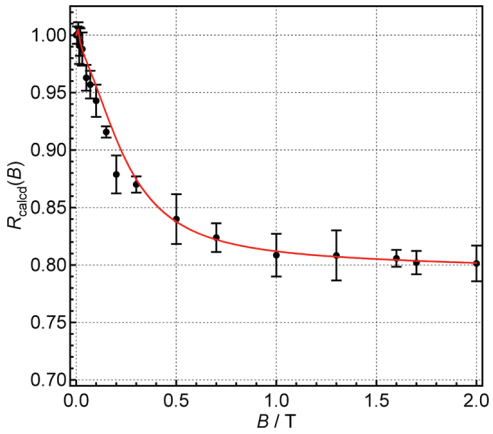

Figure 4. $R_{calcd}(B)$ calculated by the SSRP model. Parameters used in the calculations are listed in Tables 1 and 2. Filled circles are corresponding experimental results obtained in TMPA TFSA.

curve. The parameter of P_{esc} affects both shape and magnitude of the MFE in the cage model.

As you can see from the Stokes−Einstein and Stokes−Einstein−Debye relationships (eqs 6 and 7, respectively), the microviscosity in the vicinity of the RP can be estimated both from the D and τ values. Using the D value of 1.6×10^{-9} m^2 s^{-1} with the parameters of d_a = 0.4 nm, and d_b = 0.2 nm, the viscosity in the cage was estimated to be 1−2 cP from eq 6. This value is one-order of magnitude smaller than the macroviscosity (73 cP) of TMPA TFSA. The τ_b value of 5 ns on the other hand gave the viscosity of 600 cP with d_b = 0.2 nm using eq 7, which is one order of magnitude larger than the macroviscosity of TMPA TFSA. This large discrepancy between the two viscosities (1−2 cP and 600 cP) obtained by the SLE calculations cannot be explained by breaking of the Stokes−Einstein and the Stokes−Einstein−Debye relationships. Thus, the SLE calculation suggests that the IL has at least two different viscosity regions for the radical diffusions.

Wishart and Castner et al. also reported that there are several microviscosities for ILs ranging from orders of magnitude smaller than the macroscopic viscosities to viscosities larger than the macroscopic viscosities using the fluorescent probe.[39] To confirm the existence of the two viscosity regions in the IL suggested by the SLE calculation with the cage model, the SSRP model that includes the two different viscosities for the RP diffusion was applied to the SLE calculation. The Stokes−Einstein and the Stokes−Einstein−Debye relationship of eqs 6 and 7 are used to calculate the τ_a, τ_b, and D values from the η_{RP} or η_{SSRP} values. Figure 4 shows $R_{calcd}(B)$ obtained with the SSRP model. The experimental data can be reproduced by this model with the parameters of η_{RP} = 4 cP, η_{SSRP} = 2800 cP, and R = 1.9 nm. In the calculations, the SSRP with r = 1.9 nm has the longest lifetime in the RPs and $R_{calcd}(B)$ mainly reflects the S−T conversions in the SSRP with r = 1.9 nm. The lifetime (t_{SSRP}) of the SSRP was estimated to be 70 ns from the SLE calculations.[40] The rotational correlation time (τ_b^{SSRP}) for ·PhS in SSRP state was 23 ns in the calculations. The long t_{SSRP} and τ_b^{SSRP} are responsible for the saturation of the MFE at the magnetic field lower than 2 T. The parameters used in the SLE analysis are summarized in Table 2. The obtained two η values with the SSRP model are different from the macroviscosity of TMPA TFSA and represent the inhomogeneity of the solvent structure of the IL. Such inhomogeneity caused the cage effect on the RP diffusions.

In the IL, the diffusion processes of the radicals may be related with the Lévy flights[41] rather than the simple Brownian

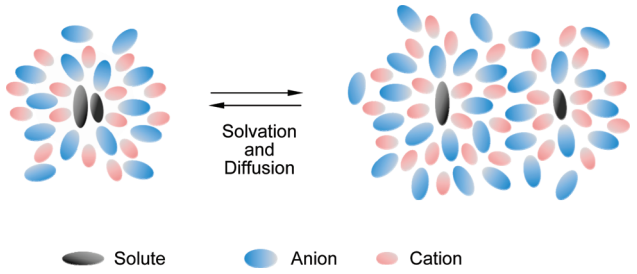

Figure 5. Schematic representations of solute diffusions and solvent dynamics after the bimolecular photochemical reaction in TMPA TFSA.

motions.[42] One of the microviscosities, which is significantly lower than the macroviscosity of IL, is considered to be related with the reported chemical reaction rate constants that are higher than the diffusion-controlled reaction rate constant predicted from the macroviscosity of ILs.[12−15] Takahashi et al. reported the high rate constant for the reactions of excited-state benzophenone ketyl radical in 1-butyl-3-methylimidazolium bis(trifluoromethylsulfonyl)amide (Bmim-TFSA) by the two-color dual-pulse laser flash photolysis.[15] They roughly estimated a microviscosity of 2 cP around the benzophenone ketyl radical in Bmim−TFSA, assuming that the observed photochemical reaction was the diffusion limited chemical reaction. This value is close to the microviscosity around the RP in the TMPA TFSA estimated from the present study. The cage effect on the diffusion of RPs suggested in the present MFE study is also consistent with time-resolved study on the bimolecular electron transfer reaction where the back electron transfer reactions were enhanced by the cage effects in ILs.[14]

Several spectroscopic and theoretical studies indicated that ILs have the nanoscale ordering structures.[8−11,43] Among them, molecular dynamics (MD) simulations and X-ray diffraction studies suggested that the alkyl side chains of ILs are aggregated, forming the isolated domain structure.[9,11,43] Such a domain structure may work as a nanoscale cage for the RP diffusion. TMPA TFSA used in the present study however does not have long enough alkyl side chains to form the cage structure with R = 1.8−1.9 nm. The long-range order for the solvent structures in the presence of the solute molecules have been reported by MD simulations and extended X-ray absorption fine structures (EXAFS).[10] The spatial distributions of the cation and anion molecules in ILs reflect the charge distribution on the solute molecules, creating the charge ordering solvent structure around the solute molecules. When the IL contains the neutral benzene molecule, for example, one finds an excess of cation above and below the negatively charged benzene ring and an excess of anions around the equator of benzene, in which the hydrogen atoms are positively charged.[44] As a result, nanoscale charge ordering is formed around the solute molecule in ILs by the solute−solvent and the solvent−solvent coulomb interactions. Nishiyama et al. also proposed the coulomb-type interaction between the benzophenone ketyl radical and ILs from transient grating study.[35]

In the present study, solute−solvent and solvent−solvent coulomb interaction may cause the long-lived SSRP state in the IL. The possible solvation scheme after the photochemical reaction is depicted in Figure 5. First, the photochemical reaction occurs at the contact pairs. After the photochemical reaction, the anion and cation molecules of ILs around the radicals are reoriented, responding to the change of the charge distribution on the solute molecules. Because the solvent structure of ILs has the ordered structure with the range of 1−2 nm around solute moleucules,[44] the most stable RP is an SSRP with r = ∼2 nm, in which the $S-T$ spin conversion is efficient due to the small J values. The SSRP having the relatively long lifetime in the IL gave the large MFE on the present reaction. In the SSRP model, the stable and slow diffusing RP with r = ∼2 nm due to the charge ordering structure in the IL is represented with the high η_{SSRP} value for the SSRP. The RPs with r < 2 nm are on the other hand unstable because the formation of the charge ordering structure around the one radical is interrupted by the similar charge ordering structure around the other radical. In the RPs with r < 2 nm, therefore, the radicals are loosely solvated and nanoscale charge ordering solvent structures are not completed around the radicals. Consequently, the radical can diffuse faster in the IL. The fast diffusion of RPs with r < 2 nm are represented with the low η_{RP} value. The RPs with r < 2 nm can be interpreted as an intermediate RP in a process for the formation of the nanoscale charge ordering solvent structures around the solute molecules. From the SLE analysis with the SSRP model, the lifetime of the nanoscale solvent structure is estimated to be 70 ns in TMPA TFSA.

CONCLUSIONS

The magnetic field effects (MFEs) observed for the hydrogen abstraction reaction between the excited triplet state of benzophenone and thiophenol in an ionic liquid of TMPA TFSA were analyzed by the stochastic Liouville equation (SLE) with the cage and solvent separated radical pair (SSRP) model. The main future of the observed MFEs is explained by the magnetic field dependent transverse spin relaxation between the S and T_0 states caused by the large anisotropy of g value of phenylthiyl radical and the slow molecular rotation of radicals in the SSRP state. We found that there are at least two different microviscosity regions in TMPA TFSA, which may be associated with the solvation dynamics of ILs. Such inhomogeneity caused the nanoscale cage effects on the translational diffusion of the RP in the present IL. The present study by the MFE probe indicates that one can probe the microviscosity in the vicinity of the RP from the D value and also from the τ values in the present photochemical reaction when the lifetime of the RP is sufficient long.

ASSOCIATED CONTENT

Supporting Information. Details of the SLE analysis. This material is available free of charge via the Internet at http://pubs.acs.org.

AUTHOR INFORMATION

Corresponding Author

*Tel: +81-48-858-3909. Fax: +81-48-858-3909. E-mail: mawakasa@chem.saitama-u.ac.jp.

ACKNOWLEDGMENT

This work was partially supported by a Grant-in-Aid for Scientific Research B (No. 2235003) from the Ministry of Education, Culture, Sports, Science and Technology of Japan.

REFERENCES

(1) Seddon, K. R. *J. Chem. Technol. Biotechnol.* **1997**, *68*, 351–356.
(2) Welton, T. *Chem. Rev.* **1999**, *99*, 2071–2083.
(3) Wasserscheid, P.; Kein, W. *Angew. Chem., Int. Ed.* **2000**, *39*, 3772–3789.

(4) Sheldon, R. *Chem. Commun.* **2001**, 2399–2407.
(5) Dupont, J.; Souza, R. F.; Saurez, P. A. Z. *Chem. Rev.* **2002**, *102*, 3667–3691.
(6) Ohno, H. *Electrochemical Aspects of Ionic Liquids*; John Wiley & Sons, Inc.: Hobeken, NJ, 2005.
(7) Antonieei, M.; Kuang, D.; Smarsly, B.; Zhou, Y. *Angew. Chem., Int. Ed.* **2004**, *43*, 4988–4992.
(8) Iwata, K.; Okajima, H.; Saha, S.; Hamaguchi, H. *Acc. Chem. Res.* **2007**, *40*, 1174–1181.
(9) Wang, Y.; Jiang, W.; Yan, T.; Voth, G. A. *Acc. Chem. Res.* **2007**, *40*, 1193–1199.
(10) Hardacre, C.; Holbrey, J. D.; Nieuwenhuyzen, M.; Youngs, T. G. A. *Acc. Chem. Res.* **2007**, *40*, 1146–1155.
(11) Pádua, A. A.; Gomes, M. F. C.; Lopes, J. N. A. C. *Acc. Chem. Res.* **2007**, *40*, 1087–1096.
(12) McLean, A. J.; Muldoon, M. J.; Gordon, C. M.; Dunkin, I. R. *Chem. Commun.* **2002**, 1880–1881.
(13) Neta, P.; Skrzypczak, A. *J. Phys. Chem. A* **2003**, *107*, 7800–7803.
(14) Paul, A.; Samanta, A. *J. Phys. Chem. B* **2007**, *111*, 1957–1962.
(15) Takahashi, K.; Tezuka, H.; Kitamura, S.; Satoh, T.; Katoh, R. *Phys. Chem. Chem. Phys.* **2010**, *12*, 1963–1970.
(16) Hamasaki, A.; Yago, T.; Wakasa, M. *J. Phys. Chem. B* **2008**, *112*, 14185–14192.
(17) Steiner, U. E.; Ulrich, T. *Chem. Rev.* **1989**, *89*, 51–147.
(18) Nagakura, S; Hayashi, H.; Azumi, T. *Dynamic Spin Chemistry*; Kodansha-Wiley: Tokyo, NY, 1998.
(19) Hayashi, H. *Introduction to Dynamic Spin Chemistry*; World Scientific: Singapore, 2004.
(20) Maeda, K.; Robinson, A. J.; Henbest, K. B.; Dell, E. J.; Timmel, C. R. *J. Am. Chem. Soc.* **2010**, *132*, 1466–1467.
(21) Wakasa, M. *J. Phys. Chem. B* **2007**, *111*, 9434–9436.
(22) Hamasaki, A.; Yago, T.; Takamasu, T.; Kido, G.; Wakasa, M. *J. Phys. Chem. B* **2008**, *112*, 3375–3379.
(23) Wakasa, M.; Yago, T.; Hamasaki, A. *J. Phys. Chem. B* **2009**, *113*, 10559–10561.
(24) Pedersen, J. B.; Freed, J. H. *J. Chem. Phys.* **1973**, *58*, 2746–2762.
(25) Pedersen, J. B.; Freed, J. H. *J. Chem. Phys.* **1973**, *59*, 2869–2885.
(26) Wakasa, M.; Nishizawa, K.; Abe, H.; Kido, G.; Hayashi, H. *J. Am. Chem. Soc.* **1999**, *121*, 9191–9197.
(27) (b) Hansen, M. J.; Pederson, J. B. *Riken Review* **2002**, *44*, 34–37.
(28) Slichter, C. P. *Principle of Magnetic Resonance*; Harper: New York, 1965.
(29) Carrington, A.; McLauchlan, A. D. *Introduction to Magnetic Resonance*; Harper: New York, 1967.
(30) Steiner, U. E.; Wu, J. Q. *Chem. Phys.* **1992**, *162*, 53.
(31) Hamasaki, A.; Sakaguchi, Y.; Nishizawa, K.; Kido, G.; Wakasa, M. *Mol. Phys.* **2006**, *104*, 1765–1771.
(32) Tarasov, V. F.; Ghatlia, N. D.; Buchachenko, A. L.; Turro, N. J. *J. Am. Chem. Soc.* **1992**, *114*, 9517–9526.
(33) In the SLE calculation, one needs to set the finite length (Δr) in r for the SSRP. We used 0.05 nm for Δr of SSRP. This means that the radical−radical distance for the long-lived SSRP is a nearly constant. The form of the diffusion matrix for the SSRP model is described in the literature.[34]
(34) Okazaki, M.; Toriyama, K. *J. Phys. Chem.* **1995**, *99*, 17244–17250.
(35) Nishiyama, Y.; Fukuda, M.; Terazima, M.; Kimura, Y. *J. Chem. Phys.* **2008**, *128*, 164514.
(36) Terazima, M.; Okamoto, K.; Hirota, N. *J. Phys. Chem.* **1993**, *97*, 13387–13393.
(37) Burkhart, R. D.; Wong, R. J. *J. Am. Chem. Soc.* **1973**, *95*, 7203–7206.
(38) Pedersen, J. B.; Hansen, M. J.; Neufeld, A. A.; Wakasa, M.; Hayashi, H. A *Mol. Phys.* **2002**, *100*, 1349–1354.
(39) Funston, A. M.; Fadeeve, T. A.; Wishart, J. F.; Castner, E. W., Jr. *J. Phys. Chem. B* **2007**, *111*, 4963–4977.
(40) The lifetime of the SSRP was estimated from the relation of $t_{SSRP} = D_{SSRP}/\Delta r^2$.
(41) Shlesinger, M. F.; Zaslavsky, G. M.; Klafter, J. *Nature* **1993**, *363*, 31–37.
(42) Habasaki, J.; Ngai, K. L. *J. Chem. Phys.* **2008**, *129*, 194501.
(43) Triolo, A.; Russina, O.; Bleif, H.-J.; Di Cola, E. *J. Phys. Chem. B* **2007**, *111*, 4641–4644.
(44) Hanke, C. G.; Johansson, A.; Harper, J. B.; Lynden-Bell, R. M. *Chem. Phys. Lett.* **2003**, *374*, 85–90.